Invited Paper

Enhanced Ad Hoc Wireless Connectivity in Complex Environment Using Small Radio Repeater Systems

Kamal Sarabandi*, Young Jun Song, and Jungsuek Oh
Radiation Laboratory, Electrical Engineering and Computer Science Department
University of Michigan, Ann Arbor, MI 48109, USA

ABSTRACT

Ad hoc communication among small robotic platforms in complex indoor environment is further challenged by three limiting factors: 1) limited power, 2) small size antennas, and 3) near-ground operation. In complex environments such as indoor scenarios often times the line-of-sight communication cannot be established and the wireless connectivity must rely on multi-path propagation. As a result, the propagation path-loss is much higher than free-space, and more power will be needed to obtain the need coverage. Near ground operation also leads to increased path-loss. To maintain the network connectivity without increasing the required power a novel high gain miniaturized radio repeater is presented. Unlike existing repeater systems, this system utilizes two closely spaced low profile miniaturized planar antennas capable of producing omnidirectional and vertical radiation patterns as well as a channel isolator layer that serves to decouple the adjacent antennas. The meta-material based channel isolator serves as an electromagnetic shield, thus enabling it to be built in a sub-wavelength size of $0.07\lambda_0^2 \times \lambda_0/70$, the smallest repeater ever built. Also wave propagation simulations have been conducted to determine the required gain of such repeaters so to ensure the signal from the repeater is the dominant component. A prototype of the small radio repeater is fabricated to verify the design performance through a standard free-space measurement setup.

Keywords: Multi-path, radio repeater, low-profile miniaturized antennas, meta-material based channel isolator

1. INTRODUCTION

1.1 Background of this study

Contrary to free-space where the link budget and the design of a wireless network is straightforward, if one wants to establish an indoor wireless communication link, many challenges have to be overcome to arrive at an optimal design with respect to power, bandwidth, and data rate. For example in an indoor environment, the lossy walls of the building highly attenuate the transmitted signal and cause strong multi-path propagation leading to deep fast fading inside a building[1,2]. These indoor propagation phenomena lead to a hard to predict signal coverage inside a building and may cause a drop of the communication link over a short distance. To overcome this, usually higher transmit power and lower data rate are budgeted for the network. Another approach to counter these drawbacks is to implement a repeater system throughout the environment for changing the communication channel. The repeater can establish an otherwise impossible communication link between the TX and RX just by placing a low-cost and easy-to-design repeater which can be active[3] or passive[4,5]. The use of a repeater system has already been investigated to some extent for the enhancement of radio links from outside a building to the inside[3,6] or to enhance wireless communication in a multipath urban propagation cell.

In this paper, the feasibility of a simple active radio repeater system with both TX and RX located indoors is investigated. Based on the physical wave propagation phenomena in buildings, the placement of such a repeater is evaluated theoretically. Both strategic positioning of the repeater and repeater specifications itself are investigated for successful coverage enhancement. The indoor wave propagation phenomena are predicted using ray-tracing, a combination of geometrical optics and the geometrical theory of diffraction, which has been used for the analysis of indoor wave propagation over decades[1,7,8]. On the basis of these theoretical results, specifications and scenarios are given for successful use of a repeater in indoor environments.

Micro- and Nanotechnology Sensors, Systems, and Applications III, edited by
Thomas George, M. Saif Islam, Achyut K. Dutta, Proc. of SPIE Vol. 8031, 803117
 · doi: 10.1117/12.885113

1.2 Benefits of the proposed Small Radio Repeater

The proposed Small Radio Repeater consists of two miniaturized planar antennas capable of supporting an omni-directional pattern and vertical polarization. Additionally, a meta-material based isolator structure is used, and active RF amplification circuitry as well as a battery is integrated into the radio repeater platform. Since TX/RX of the proposed repeater shows omni-directional radiation pattern in H plane, the uplink and downlink signal paths can be established through a single circuit path. This can reduce complexity and power consumption of RF circuitry. In addition, pure vertical polarization allows for a simple antenna structure for the base station and end-node / units as well as a decreased path-loss along the channel. It is well understood that for near-earth wave propagation scenarios vertically polarized waves experience much less path-loss compared to horizontally polarized waves[9]. To achieve the compact dimension of the radio repeater, a meta-material based channel isolator is utilized. By generating the normal magnetic field along the signal path between TX and RX, artificial magnetic walls are generated that serve to suppress the electromagnetic wave propagation from TX to RX antennas. The proposed radio repeater occupies a very small area ($0.07\ \lambda_0^2$) with a very short height ($\lambda_0/70$) without its active circuitry. The passive components such as two miniaturized antennas and meta-material based isolator are presented and verified in this paper. The prototype is fabricated using a commercially available dielectric substrate. In addition, a commercially available RF amplifier and battery are used to verify the operational feasibility of the proposed repeater. This configuration is shown to boost the power level of the received signal by 32 *dB*.

2. INDOOR WAVE PROPOAGATION ASSISTED BY RADIO REPEATERS

2.1 Concept of Radio Repeater

The radio repeater system is designed to amplify and transmit a predetermined received signal. A series of repeaters are capable of relaying information in stringent wireless propagation environments by forming an ad-hoc network. A rudimentary figure of the radio repeater is shown in Fig. 1.

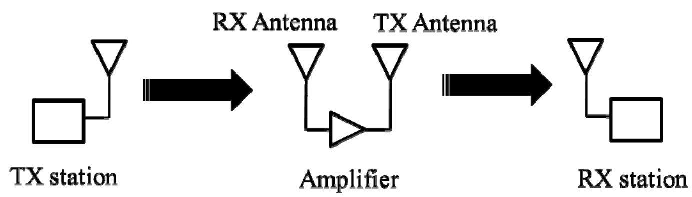

Fig. 1. Radio repeater system configuration.

The radio repeater establishes a LOS communication link between the TX and RX station. To explain the concept, let us imagine a simple scenario where a direct communication link between TX and RX is blocked by a wall. In this case, the signal coverage is established via penetration through the wall and diffraction from the edges of the wall, with both signal paths highly attenuated. By utilizing the radio repeater at the appropriate position, a direct communication link is formed and thus signal coverage can be improved as depicted in Fig. 2.

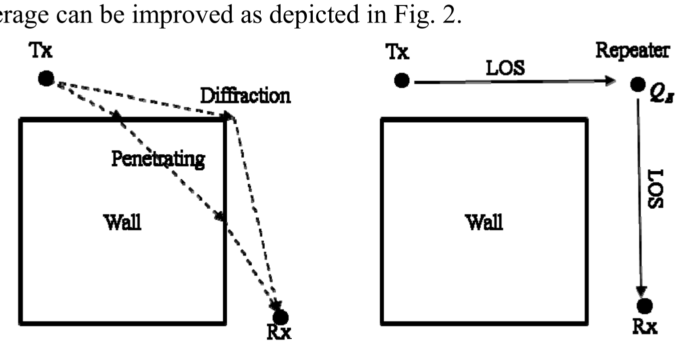

(a) (b)

Fig. 2 Concept of radio repeater placement: (a) without and (b) with a repeater

2.2 Formulation of Power Enhancement with a Repeater System

As a simplification, the wave propagation using a repeater is explained by applying the Friis formula, assuming LOS between the repeater and both TX and RX. First, the repeater acts as an RX and the Friis formula is applied once to find the received power at the repeater position. This power is amplified and retransmitted and Friis formula is applied a second time to find the received power at the RX position. The equation below shows this process.

$$\begin{aligned}\frac{P_r}{P_t} &= \frac{G_t G_{ant} \lambda^2}{(4\pi R_1)^2} G_{amp} \frac{G_{ant} G_r \lambda^2}{(4\pi R_2)^2} \\ &= (G_t G_r) \frac{\lambda^2}{(4\pi R_1)^2} \frac{\lambda^2}{(4\pi R_2)^2} (G_{rep}) \end{aligned} \tag{1}$$

where P_t and P_r are the transmitted and received power, G_t and G_r are the gain of TX/RX Antenna, G_{ant} and G_{amp} are the gain of TX/RX Antenna and Amplifier in repeater, $G_{rep} = G_{ant}^2\, G_{amp}$ is the total gain by repeater.

It is assumed that the repeater simply consists of one TX and one RX antenna with one amplifier in between. It should be noted that when wave propagation goes through the repeater, the attenuation due to $\lambda^2/(4\pi)^2$ as well as the gain due to G_{Rep} is added. In an indoor environment, the free-space path loss $\lambda^2/(4\pi R)^2$ has to be replaced with the actual measured or estimated path loss *PL*. Now the direct path loss and the path loss with the repeater system can be compared:

1) Direct link

$$\frac{P_r}{P_t} = G_t G_r PL_{t\to r} \tag{2}$$

2) Through repeater

$$\frac{P_r}{P_t} = G_t G_r G_{rep} PL_{t\to rep} PL_{rep\to r} \tag{3}$$

Consequently, in order to enhance the signal coverage with a repeater, the following equation has to be met

$$G_{rep} PL_{t\to rep} PL_{rep\to r} > PL_{t\to r} \tag{4}$$

where $PL_{t\to r}$ is the path loss from TX to RX, $PL_{t\to rep}$ the path loss from TX to the repeater and $PL_{rep\to r}$ the path loss from the repeater to RX.

2.3 SIMULATION OF REPEATER IN INDOOR SCENARIOS

As introduced in Section 2.1, the use of a repeater is most effective when the direct path between the TX and RX is blocked and the repeater can install a LOS, therefore these scenarios are investigated. In this case the direct communication link between TX and RX is blocked by walls and the signal coverage is only established via highly attenuated penetration through the walls or low power diffraction from the edges of the walls.

The simplest possible scenario is a corner of two impenetrable walls (as shown in Fig. 2, omitting transmitted ray) which has the highest possible path loss without repeater system and is hence the ideal scenario for a repeater placement. However, since an indoor scenario is never formed of a single corner but of multiple rooms, hallways and hallway junctions, the path loss around realistic hallway junctions needs to be investigated. Therefore, a Shoot-and-Bounce ray-tracing approach is applied to various hallway junctions shown in Fig. 3. The ray-tracing method also includes diffraction at the hallway corners, calculated with the geometrical theory of diffraction with a heuristic adjustment of the diffraction coefficients for dielectric materials[10]. The path loss was computed along the path R2 of Fig. 3 with a distance of 11m between the TX and the hallway junction at 2.4 *GHz*, omitting wall penetration. The TX is 11m away from the junction and the dielectric constant of the wall is 4.8 with a conductivity of 0.02 *S/m*, representing concrete.

Fig. 4(a) shows the path loss of all hallway junctions compared to the diffraction around a single corner. The received field in non-LOS hallways is about 30 *dB* higher than in the single diffraction case. This is due to multiple wall reflections in the hallway to and edge diffraction. While the edge diffraction due to the shortest path (without wall reflections) in hallway is very weak, the edge diffraction of a multiple reflected ray is strong leading to a higher received field (compare Fig. 4(b)).

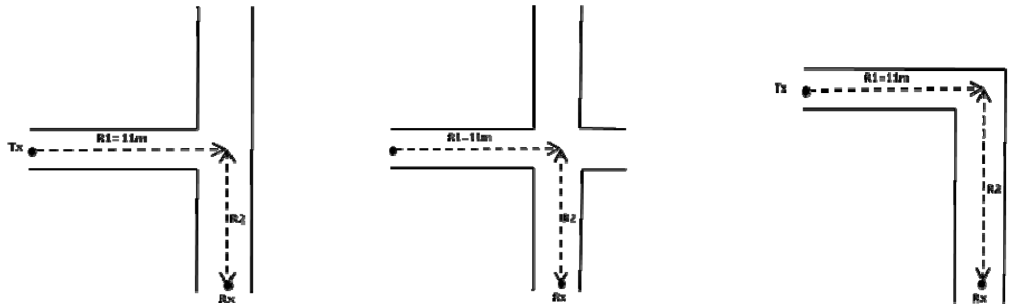

(a) (b) (c)

Fig. 3. Possible hallways junctions: (a) T-type, (b) X-type, and (c) L-type

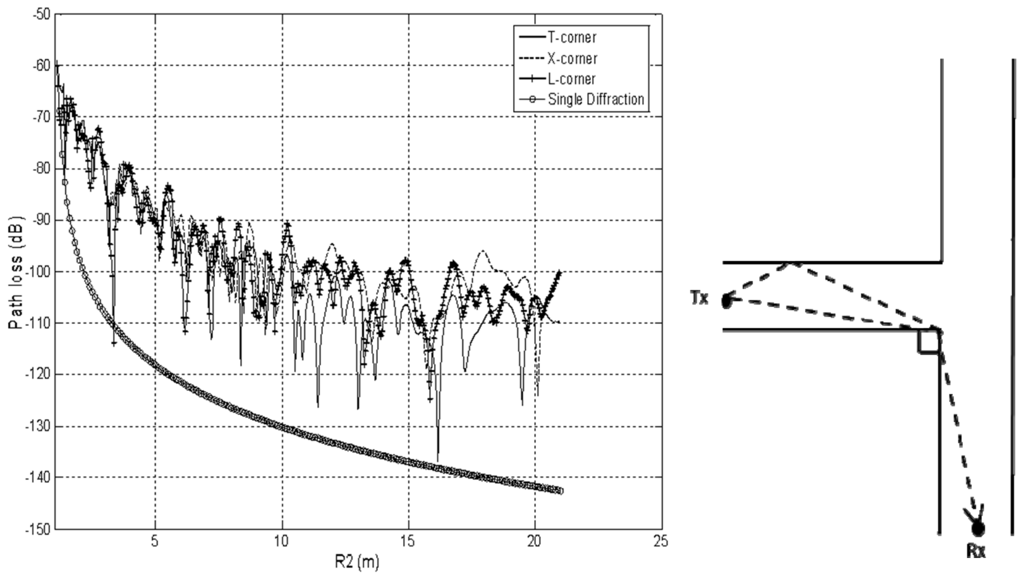

(a) (b)

Fig. 4. (a) The path loss along the hallway of Fig. 3 at 2.4 *GHz* and (b) Multiple diffracted rays in the T-type hallway

Now the placement of the radio repeater in the hallway junction can be considered and coverage enhancement based on the overall repeater gain can be analyzed. For simplification, the path loss along the hallway is compared with LOS from the TX to the repeater and from the repeater to the RX. Fig. 5 shows the resulting path loss due to wave propagation using the radio repeater for various repeater gain numbers (10 *dB*, 20 *dB* and 30 *dB*). Although it neglects the fast-fading effects of the hallway that add to the LOS path, it is a good estimation of the field coverage through the repeater and indicates that an employment of the radio repeater is advantageous for gain value greater than 20 *dB*. For example, 30 *dB* Gain achieves about 10 *dB* margin, compared to the coupling at the hallway junction.

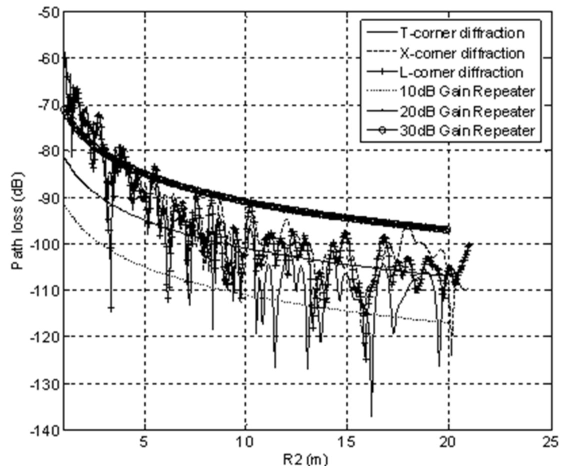

Fig. 5. The path loss along the hallway of Fig. 4 at 2.4 *GHz* compared to path loss of LOS propagation through repeater placed at the hallway junction.

3. DESIGN SPECIFICATION OF SMALL RADIO REPEATER

3.1 Miniaturized Low-profile planar Antenna

The radiation properties of antenna are mainly determined by magnitude and direction of current distribution over the antenna itself. In many practical miniaturized antennas, an impedance mismatch causes limitation of the excited current and degradation of antenna performance. To achieve a good input impedance matching in a low-profile miniaturized antenna, a quarter-wave microstrip resonator fed near short-circuited end can be used[11]. Although a good reflection coefficient can be obtained with this method, this approach requires two layers which cause fabrication complexity and potential risk of frequency shift due to misalignment. In order to address these problems, it was proposed to place the matching network at the same layer of the miniaturized antenna as shown in Fig. 6. Although the vertical polarized radiation is mainly originated from the shorted pins, some horizontal polarized radiation is emanated from the spiral arms. Therefore, by placing each of the spiral arms in a symmetrical manner the horizontally polarized radiated field can be cancelled, and eventually an omni-directional vertically polarized radiation pattern can be achieved.

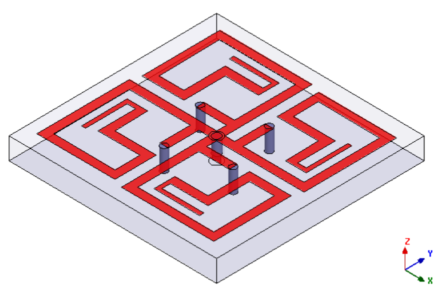

Fig. 6. Topology of optimized Multi-element Monopole Antenna (MMA)

To be incorporated into the sub-wavelength dimension of the proposed radio repeater, the optimized MMA was further modified. Since a pair of four arms can produce a high level of mutual coupling within the small distance, two arms of the optimized MMA were removed at the expense of asymmetric radiation pattern in E plane as shown in Fig. 7. As can be seen in Fig. 8, the modified MMA is well matched with -18.5 *dB* of input reflection coefficient and maintains the omni-directional vertical polarized pattern in the H-plane.

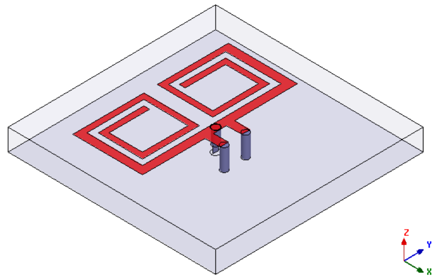

Fig. 7. Topology of modified MMA for Small Radio Repeater

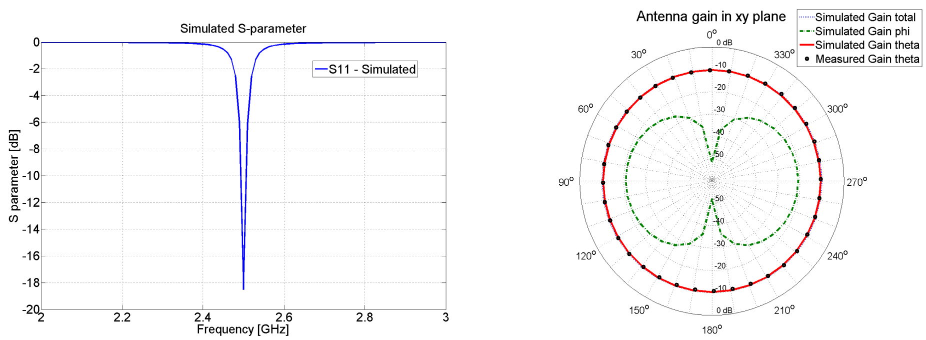

(a) (b)

Fig. 8. Simulated responses of Modified MMA: (a) S_{11} response and (b) Radiation pattern in H(xy) plane

3.2 Meta-material based Resonant Channel Isolator

In sub-wavelength dimensions, mutual coupling between two antennas becomes the most critical factor to impede a compact integration of system. In order to achieve the miniaturization of system, the mutual coupling should be suppressed. Thus meta-material insulator was proposed to prevent EM energy from being transmitted across the insulation boundary[12]. However, in order to relieve fabrication complexity and cost of this approach, a new meta-material based channel isolator was proposed and designed as shown in Fig. 9[13]. The proposed isolator was designed to resonate at the desired channel frequency and suppress the surface mode generated by the vertical pins of the modified MMA. Since the vertical pins create a Transverse Magnetic (TM) wave in the substrate with zero cutoff frequency, the magnetic field is parallel to the ground plane and perpendicular to the vertical pins of the proposed channel isolator. This horizontally polarized magnetic field is linked by the square loop and induces an electric current on the vertical wires. In addition, this induced current generates a magnetic field which is perpendicular to the loop of the channel isolator. When the unit cells are closely spaced to each other, the inductance of the loops is increased and the periodic array acts like a solenoid. Thus, at resonance the periodic layer behaves as a Perfect Magnetic Conductor (PMC) plane. Due to the mutual coupling of the adjacent loops, the self inductance of the square loop as shown in Fig. 9(a) can be obtained from[14]

$$L_s = \frac{\mu_r \mu_o A_{loop}}{d} \tag{5}$$

where $A_{loop} = h\, l_{loop}$ is the internal area of the loop, and d the periodicity of unit cells.

In order to generate the resonance, the lumped capacitor can be realized by an interdigital capacitor as shown in Fig. 9 (b). The current induced by the magnetic field transforms to a displacement current as it gets through the gaps between the series interdigital strips, in turn, it acts like a distributed capacitor. Since the most of electric field are confined between the interdigital strips, its capacitance can be computed based on conformal mapping given by[15]

$$C_{i,e} = \varepsilon_r \varepsilon_o \frac{K(k_{i,e})}{K(\sqrt{1-k_{i,e}{}^2})} \tag{6}$$

$$k_i = \sin(\frac{\pi}{2}\eta) \text{ and } k_e = 2\frac{\sqrt{\eta}}{1+\eta} \tag{7}$$

where $\eta = w/(w + g)$ is the metallization ratio and $K(k)$ is the complete elliptic integral of first kind defined by

$$K(k) = \int_0^{\pi/2} \frac{d\phi}{\sqrt{1-k^2 \sin^2 \phi}} \tag{8}$$

Since the individual capacitors between fingers are connected in parallel, the total capacitance per unit length of interdigital capacitor is equal to

$$C_{unit} = (n-3)\frac{C_i}{2} + 2\frac{C_i C_e}{C_i + C_e} \quad \text{for n > 3} \tag{9}$$

where C_i is the capacitance between inner strips, C_e is between outer and inner strips, and n is the number of strips. Hence, the total capacitance of the proposed isolator can be calculated easily from $C_s = C_{unit}\, l_{cap}$, where l_{cap} is the length of the interdigital strips. The designed parameters are summarized in Table 2. The corresponding inductance and capacitance of the unit cell are thus found to be 15.2132 *nH* and 0.1869 *pF*, respectively.

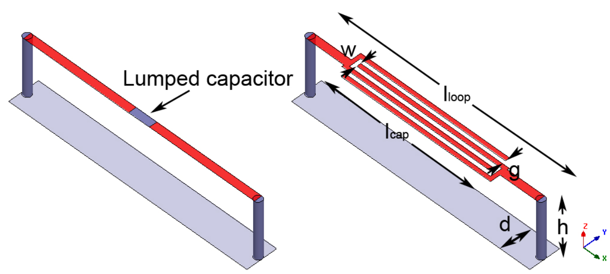

(a) (b)

Fig. 9. Unit cell of channel isolator: (a) Channel Isolator and (b) topology of unit cell using interdigital capacitor

Table 2. Designed parameters of Meta-material based Channel Isolator.

Design parameter	**Dimension**
l_{loop}	6.25 *mm*
l_{cap}	3.84 *mm*
g	0.10 *mm*
w	0.10 *mm*
h	1.57 *mm*
d	0.81 *mm*
n	4

3.3 Integration of Two Miniaturized Antennas and Channel Isolator

The proposed radio repeater is composed of two miniaturized low-profile antennas capable of radiating vertical polarization and a meta-material based channel isolator as shown in Fig.10. Since a close spacing between the antennas and the isolator causes the interaction, it affects the electrical properties of the repeater such as the antenna input impedance and the resonant frequency of the isolator. As all of the physical parameters are related to each other through electromagnetic interactions, system integration was performed through adjusting the design parameters of the isolator iteratively. All design parameters were optimized for the repeater to operate around 2.72 *GHz* and are reported in Table 3.

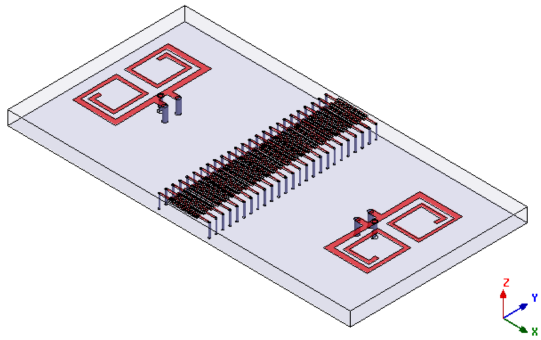

Fig. 10. Repeater platform without channel isolator: 3D view

Table 3. Designed parameters of Small Radio Repeater.

Design parameter	Dimension
Distance between two Antennas	24.99 *mm*
Distance between two vertical wires (l_{loop})	5.84 *mm*
Length of strip fingers (l_{cap})	3.38 *mm*
Width of platform	20.68 *mm*
Length of platform	40.01 *mm*
Height of platform	1.57 *mm*

4. VERIFICATION OF SMALL RADIO REPEATER

4.1 Full wave simulation of Small Radio Repeater

The designed small radio repeater was analyzed using commercial full-wave simulation. The simulated S-parameters of the optimized small radio repeater are reported in Fig. 11. As shown, in the presence of the antenna, the resonance of isolator occurs at 2.72 *GHz*, and the transmission coefficient was dropped from -20 *dB* to -30 *dB* with incorporating the channel isolator. The magnetic field distributions over the ground plane with and without the isolator were investigated to determine the operation of the proposed channel isolator. As expected, the horizontal magnetic field generated from the TX propagates through the substrate and causes the mutual coupling to the RX. When incorporating the channel isolator, the horizontal magnetic field is maximized within the channel isolator, which implies that the mutual coupling was suppressed through the channel isolator.

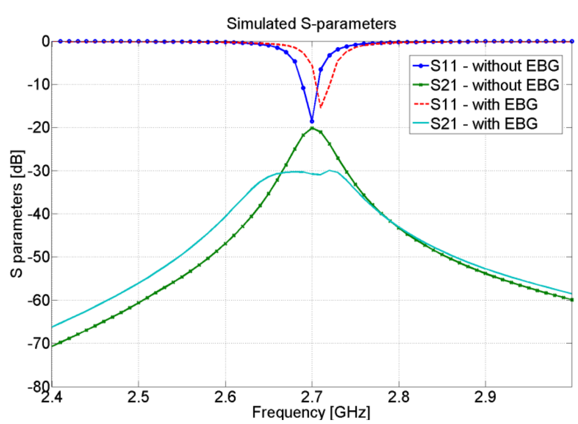

Fig. 11. Simulated S-parameters of the Small Radio Repeater with and without the meta-material isolator

4.2 Experimental result of fabricated Small Radio Repeater

The prototype of the proposed small radio repeater was fabricated using a commercial substrate ($\varepsilon_r = 2.2$). As can be seen in Fig. 12, the repeater without the channel isolator shows -18 *dB* of transmission coefficient, and the proposed repeater shows -42 *dB* of transmission coefficient, which indicates 24 *dB* of improvement at the resonant frequency. Although -28 *dB* of peak level of *S*21 is observed, a maximum gain of 32 *dB* for a wideband RF amplifier can be utilized with this repeater. Since the antennas are slightly mismatched near to the operation frequency, the maximum gain can be slightly higher than the peak level of *S*21. Thus, it is convinced that a RF amplifier with 32 *dB* of gain can be integrated into the proposed small radio repeater without oscillation.

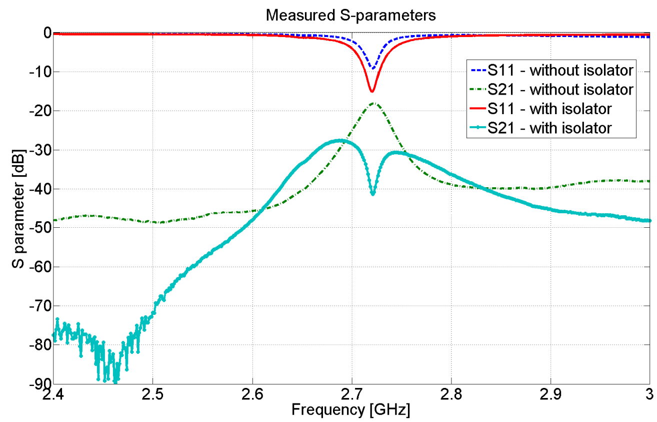

Fig. 12. Measured S-parameters of proposed Small Radio Repeater

5. CONCLUSION

In this paper, a new concept for implementation of miniaturized radio repeater is presented. To construct the radio repeater, two miniaturized low-profile antennas ($\lambda_0/70$) radiating vertical polarization and a very thin meta-material isolator layer are integrated into a compact dimensions. The antennas are designed to have an omni-directional radiation pattern to make the repeater insensitive to the positions of the transmitter and receiver. In addition, the proposed isolator is shown to suppress the mutual coupling, improving the transmission coefficient from -18 *dB* to -42 *dB*. The overall dimensions of the proposed radio repeater are 40.01 *mm*×20.68 *mm*×1.57 *mm*, which corresponds to $\lambda_0/2.75\times\lambda_0/5.32\times\lambda_0/70$. The proposed radio repeater system has been simulated and verified experimentally. The prototype of the design has been fabricated using printed circuit technology, which serves to reduce fabrication complexity and allows for easy commercial production at a large scale.

As mentioned in Section 2, at least G_{rep} = 30 *dB* of repeater gain is anticipated to observe the merit of Small Radio Repeater. Although the proposed radio repeater can be incorporated with 32 *dB* of RF amplifier gain, improvement of TX and RX gain is still required to meet the system criteria. Since the gain of small antenna is mostly determined by conducting loss, the current distribution of antenna structure and electric/magnetic field confinement should be optimized to increase the antenna gain. In addition, it was observed that the induced electric current over the ground plane also causes the mutual coupling between two antennas and quarter wavelength of electric chokes can suppress this induced current. The further improved repeater system will be presented at the conference.

REFERENCES

[1] Fuegen, T., Maurer, J., Kayser, T., and Wiesbeck, W., "Capability of 3-D Ray Tracing for Defining Parameter Sets for the Specification of Future Mobile Communications Systems," *IEEE Trans. Antennas Propag.* **54**(11), 3125-3138 (2006).

[2] Schaefer, T. M., and Wiesbeck, W., "Simulation of Radiowave Propagation in Hospitals Based on FDTD and Ray-Optical Methods," *IEEE Trans. Antennas Propag.* **53**(8), 2381-2388 (2005).

[3] Slobodrian, P. M., "Estimation of the repeater gain required for a wireless link," 15th Int. Conf. on Microwave Radar and Wireless Commun. MIKON, (2004).
[4] Hristov, H., Feick, R., and Grote, W., "Improving indoor signal coverage by use of through-wall passive repeaters," Int. Symp. on Antennas and Propagation, (2001).
[5] Huang, Y., Yi, N., and Zhu, X., "Investigation of using passive repeaters for indoor radio coverage improvement," Int. Symp. on Antennas and Propagation, (2004).
[6] Naemat, A. H., Tee, A., Marzuki, A. S. M., Mohmd, B., Khalil, K., and Rahim, A. R. A., "Achieving Optimum in-building Coverage of 3G Network in Malaysia," Proc. of int. RF and Microwave conf., Putraja, Malaysia, (2006).
[7] Iskander, M. F., and Yun, Z., "Propagation prediction models for wireless communication systems," *IEEE Trans. Microw. Theory Tech.* **50**(3), 662-674 (2002).
[8] Seidel, S. Y., and Rappaport, T. S., "Site-specific propagation prediction for wireless in-building personal communication system design," *IEEE Trans. Veh. Technol.* **43**(4), 879-892 (1994).
[9] Liao, D., and Sarabandi, K., "Terminal-to-Terminal Hybrid Full-Wave Simulation of Low-Profile, Electrically-small, Near-Ground Antennas," *IEEE Trans. Antennas Propag.* **56**(3), 806-814 (2008).
[10] Burnside, W. D., and Burgener, K. W., "High frequency scattering by a thin lossless dielectric slab," *IEEE Trans. Antennas Propag.* **31**(1), 104-111 (1983).
[11] Hong, W., and Sarabandi, K., "Low-profile, Multi-element, Miniaturized Monopole Antenna," *IEEE Trans. Antennas Propag.* **57**(1), 72-80 (2009).
[12] Buell, K., Mosallaei, H., and Sarabandi, K., "Metamaterial Insulator Enabled Superdirective Array," *IEEE Trans. Antennas Propag.* **55**(4), 1074-1085 (2007).
[13] Sarabandi, K., and Song, Y. J., "Subwavelength Radio Repeater System Utilizing Miniaturized Antennas and Metamaterial Channel Isolator," *IEEE Trans. Antennas Propag.*, accepted for publication, (2011).
[14] Mosallaei, H., and Sarabandi, K., "Design and Modeling of Patch Antenna Printed on Magneto-Dielectric Embedded-Circuit Metasubstrate," *IEEE Trans. Antennas Propag.* **55**(1), 45-52 (2007).
[15] Igreja, R., and Dias, C. J., "Analytical evaluation of the interdigital electrodes capacitance for a multi-layered structure," *Sensors and Actuators A: Physical* **112**, 291-301 (2004).